 doi:10.20944/preprints202207.0163.v1

Article

A step-wise modelling approach to identifying structural features that control groundwater flow in a folded carbonate aquifer system

Elisabetta Preziosi[1], Nicolas Guyennon[1], Anna Bruna Petrangeli[1], Emanuele Romano[1] and Cristina Di Salvo[2,*]

1 CNR-Water Research Institute; elisabetta.preziosi@cnr.it; guyennon@irsa.cnr.it; petrangeli@irsa.cnr.it; emanuele.romano@irsa.cnr.it
2 CNR-Institute of Environmental Geology and Geoengineering ; cristina.disalvo@igag.cnr.it
* Correspondence: cristina.disalvo@igag.cnr.it

Abstract: This paper concerns about a stepwise modelling procedure for groundwater flow simulation in a complex carbonate, folded and faulted, multilayer aquifer, in the Apennine chain in Central Italy, which constitutes a source of good quality water for human consumption. A perennial river acts as the main natural drain for groundwater while sustaining valuable water related ecosystems. The spatial distribution of recharge was estimated using the Thornthwaite-Mather method on 60 years of climate data. The system was conceptualized as three main aquifers separated by two locally discontinuous aquitards. Three numerical models were implemented by gradually adding complexity to the model grid: single layer (2D), three layers (Quasi-3D), and five layers (Fully-3D), using an equivalent porous medium approach, in order to find the best solution with a parsimonious model setting. To overcome dry-cell problems in the Fully-3D model, the Newton-Raphson formulation for MODFLOW-2005 was invoked. Calibration results show that a Fully-3D model was required to match the observed distribution of aquifer outflow to the river baseflow. The numerical model demonstrated the major impact of folded and faulted geological structures on controlling the flow dynamics in terms of flow direction, water heads and spatial distribution of the outflows to the river and springs.

Keywords: Carbonate aquifer, groundwater modelling, multilayer aquifer, MODFLOW-NWT formulation, Central Italy.

1. Introduction

Carbonate aquifers are important groundwater resources worldwide, due to their high permeability and rapid groundwater velocities. Ford and Williams [1] estimate that 20% of the world population largely depends on groundwater from carbonate aquifers. These are often as defined karst aquifers, due to their "self-organized, high permeability channel networks formed by positive feedback between dissolution and flow" ([2]). An important feature of the carbonate aquifers, especially when diffuse flow prevails, is their capability to store huge quantities of groundwater during humid periods and gradually release them during dry periods. Hence, they are fundamental to sustain both human uses and groundwater-related ecosystems in many parts of the world. Water quality in carbonate aquifers is often excellent; hence, they are regarded as strategic both for human consumption as well as to sustain the environmental uses. The high permeability often results in thick unsaturated zones, so exploitation of groundwater is often from low-elevation springs, especially in mountainous areas ([3]). Pumping wells located near the springs are used to overcome spring discharge shortage in dry seasons ([4]).

These resources are very often exploited to supply large urban areas, and the evaluation of the possible negative effects of climate changes on their discharge is challenging. The decrease in annual precipitation and increase in temperature and evapotranspiration

Preprints (www.preprints.org) | NOT PEER-REVIEWED | Posted: 11 July 2022 doi:10.20944/preprints202207.0163.v1

due to climate change in the Mediterranean area ([5]-[9]), is leading to a general decline both in surface water discharge ([10]) and in recharge to groundwater ([11]). Preziosi and Romano, 2013[12] highlighted that spring discharge of large carbonate aquifers in central Italy has decreased by 6% to 42% in the period 1938-2011, the highest percentages estimated for the smallest springs ([13]).

The development of numerical models is considered a fundamental step for the adoption of water management plans aiming to preserve groundwater resources and the related ecosystems ([14]). Many authors have focused on the numerical modelling of karst systems to assess the risk of spring discharge shortage due to climate change ([15]; [16]), or to evaluate the effects of withdrawals ([4]). However, numerical modeling of carbonate aquifers in folded and faulted terrains is a hard challenge, due to the complexity of the hydrogeological systems, and an excessive simplification may lead to an unsatisfactory predictive capability of the model. Carbonate aquifers are often characterized by highly conductive conduit flow paths embedded in a less conductive fissured and fractured matrix ([17]In spite of these strong permeability contrasts, the Equivalent Porous Medium approach (EPM) can be applied to karstified aquifers with some limitations; specifically, it often fails to predict flow direction and velocity but it can correctly approximate flow and spring discharge at the regional scale ([18]). Further, Abusaada and Sauter, 2013 [19] affirm that EPM models can simulate flow in karst aquifers as long as the simulated saturated volume is large enough to average out the local influence of karst conduits.

The significant influence of the geological structure (especially folding and lithology) and the karst system on the location of the springs and their flow regime has been addressed by [20] and [21]. Structural folds may divert groundwater flow from the general hydraulic gradient; the presence of marly layers may sustain perched sub-aquifers above the regional aquifer; karstification may locally increase the hydraulic conductivity by several orders of magnitude. Moreover, complex geometry of model layers can result in different thicknesses of saturated portions, which can imply drying and rewetting of cells during model iterations, leading to numerical instabilities, preventing convergence or increasing numerical error ([22]). Including all these characteristics in the conceptual and numerical model requires the adequate definition of layer thickness, dipping, and hydraulic properties.

Recent advances in groundwater numerical modeling include the development of solvers which facilitate achieving convergence and/or reduce computational errors due to model nonlinearities, as well as packages tailored for solving specific problems ([23]). This allows the development of Fully-3D numerical models, able to reproduce complex settings with stable solutions. However, by increasing model structure complexity, the number of input parameters increases, as well as the related uncertainty. A model with too many parameters is susceptible to over-fit the data ([24]-[26]). The higher is the complexity, the more accurate should be the calibration procedure, this requiring an adequate number of calibration targets. Simulating complexity not supported by the data can be useless and misleading.

The aim of this research was to develop and test a modelling procedure for the simulation of groundwater flow in a complex karst, folded, multilayer aquifer using the EPM approach. In this framework, three steady-state numerical models of a carbonate aquifer in Central Italy (Monte Coscerno) were developed with increasing complexity as warranted by the inability of the model to adequately reproduce observations ([27]). A stepwise procedure was developed for testing the ability of the models to reproduce observations. Seeking for parsimony, we compare the results from a simple 1-layer model and more complex Quasi-3D and Fully-3D models, with different number of layers and parameters' spatial variability.

2. Conceptual model

2.1 Geological and hydrogeological setting

Preprints (www.preprints.org) | NOT PEER-REVIEWED | Posted: 11 July 2022 doi:10.20944/preprints202207.0163.v1

The case study aquifer (Monte Coscerno, 230 km²) is located in the Apennine chain in Central Italy (Figure 1). It can be described as a box-fold anticline with a meridian axis ([28]). The main tectonic thrusts, mainly with a meridian direction, bound nearly all the aquifer (black solid line in Figure 1), and act as no flow boundary. The general groundwater flow is mainly in a south to north direction, parallel to the prevailing tectonic lines ([29]-[31]). A sequence of Meso-Cenozoic calcareous formations interbedded with marly formations results in a multilayer aquifer, with three main sub-aquifers (from bottom to top: Calcare Massiccio-Corniola, Maiolica, Scaglia limestone units) separated by two aquitards ([30]). The aquitards can be locally discontinuous, due to depositional, erosional and tectonic effects, favouring vertical leakance between the three aquifers ([31];[32]). The base of the aquifer is represented by the top of the Triassic dolomitic evaporitic complex ("Marne a Rhaetavicula contorta" marlstones and "Anidriti di Burano" anhydrites, ([33];[31]), mostly dipping westward. Groundwater is expected to flow according to the layering, in the direction of the steepest descent. This may result in large unsaturated portions in the eastern part of the aquifer (Figure 2); moving westward, the sub-aquifers 2 and 3 become confined, feeding the Scaglia sub-aquifer through vertical leakance upward. The sub-aquifers 1 and 2 do not extend through all the model area, due to erosional processes which affected the anticline eastside where the more ancient formations outcrop (Figure 1 and Figure 2); for this reason, rainfall infiltrates through the uppermost outcropping aquifer and flows westward and northward, according to the dip of the layers.

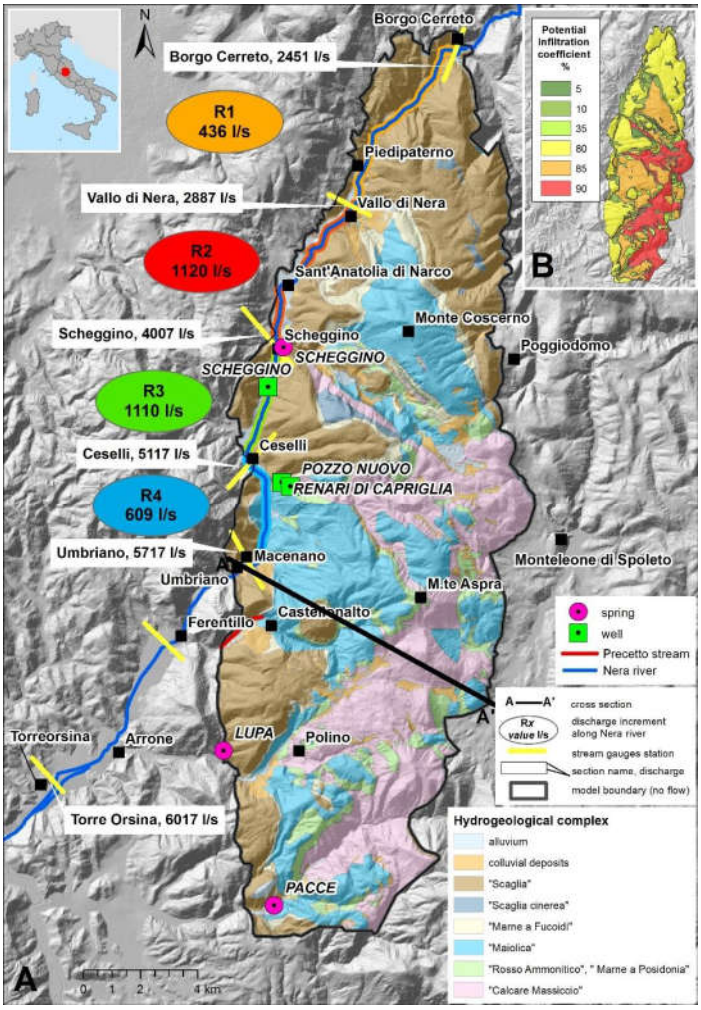

Preprints (www.preprints.org) | NOT PEER-REVIEWED | Posted: 11 July 2022 doi:10.20944/preprints202207.0163.v1

Figure 1. A: Hydrogeological setting, conceptual model. B: distribution map of the potential infiltration coefficients.

Hourly hydrometric data and periodic discharge measurements of Nera River in two stream gauging stations (Vallo di Nera and Torre Orsina, Figure 1) have been made available by the Umbria Region since 2006. The monthly discharge of Lupa spring was available for the period 1985-1997. Moreover, Lupa spring daily discharge (since 1998) and piezometric heads measured in Scheggino well (since 2001) are available on-line from the local Regional Environmental Agency ([34]). Head data are very scarce, except for the already mentioned Scheggino well and the very recently excavated Renari di Capriglia well (Figure 1). The Nera River cuts the carbonate aquifer, increasing its discharge from north to south. Several discharge measurements performed in the years 1991-1993 at the 6 gauging stations in Figure 1 ([35]) indicate a conspicuous discharge increment, nearly constant throughout the year, revealing gaining stream conditions between Vallo di Nera and Umbriano (reaches R1 to R4, fig.1). The river baseflow was estimated between 3.2 and 3.4 m^3/s in the period 1991-1993 by Boni and Preziosi, 1993[29]. In addition, the aquifer feeds several point springs (Scheggino, Lupa and Pacce) and the Precetto stream (Figure 1, Table 1).

Table 1. Gauging stations and springs in the study area.

Site name	altitude (m a.s.l.)	Average discharge (L/s)	Reference period	Reference
Borgo Cerreto	345	2451	1991-1993	[30]
Vallo di Nera	293	2887	1991-1993	[30]
Scheggino	275	4007	1991-1993	[30]
Ceselli	265	5117	1991-1993	[30]
Umbriano	242	5717	1991-1993	[30]
T.Orsina	211	6017	1991-1993	[30]
Scheggino spring	276	190	1991-1993	(accounted for in the Ceselli gauging site) [30]
Lupa spring	366	120	1997-2012	[34]
Pacce spring	480	60	2000-2001	Well field excluded. [36]
Precetto stream	325	120	1991-1993	[30]
Borgo Cerreto	345	2451	1991-1993	[30]
Vallo di Nera	293	2887	1991-1993	[30]

The aquifer discharge to the Nera River in the years 1997-2012 was estimated as the discharge increment between two gauges (Vallo di Nera and Torre Orsina gauges, Figure 1) using spot measurements provided by the Regional Environmental Agency ([34]). The average of the 83 spot measurements is 3.28 m^3/s, ranging from 0.9 to 7.46 m^3/s (Figure 3). The total aquifer discharge was estimated about 3.4-3.6 m^3/s, with an extremely regular regimen, uncommon in karst areas ([35]). However, there is no evidence in the area of developed karst conduits, despite the presence of likely fractured limestones. Consequently, Monte Coscerno can be classified as a "diffuse flow aquifer" ([37]), i.e. a carbonate aquifer system with dispersive circulation, due to a micro-fractured interconnected network, with extremely reduced or even inexistent karstification, without preferential drainage paths ([38]).

Preprints (www.preprints.org) | NOT PEER-REVIEWED | Posted: 11 July 2022 doi:10.20944/preprints202207.0163.v1

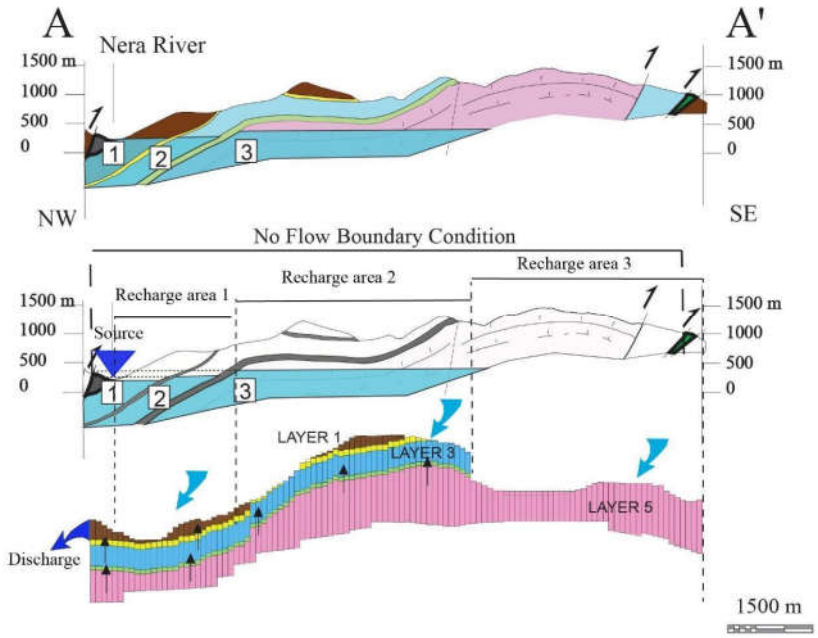

Figure 2. Schematic cross section and translation into model grid for the Fully-3D model. Trace of cross section and legend are in Figure 1.

2.2 Recharge estimation

Daily precipitation and mean temperature (period: 1950-2013) were collected over the case area at 16 and 7 station locations respectively. Data were interpolated over a 1 km^2 regular grid through an Ordinary Kriging. Temperature data were previously detrended from the local lapse rate. Observed semi-variograms were fitted through a spherical model at a monthly time step. The recharge to the aquifer was estimated, at a daily time step, by using the Thornthwaite-Mather model ([39],[40]). Recharge is assumed to be the fraction of water surplus when soil moisture exceeds the field capacity. Soil moisture was estimated as the difference between precipitation and actual evapotranspiration, the latter computed as a fraction of the potential evapotranspiration when the soil is partially saturated. Field capacity (set to 100 mm, [30]) and infiltration coefficients ranging from 5 to 90% of the precipitation (ascribed to each hydrostratigraphic unit on an expert judgment basis, Figure 1b), have been calibrated to match the observed aquifer contribution to the river and springs (3.4-3.6 m^3/s). The average estimated infiltration rate after calibration is 480 mm/y, corresponding to an average discharge of 3.5 m^3/s. Non-stationarity in the estimated recharge was assessed through a singular spectrum analysis (SSA) for the past 60 years (1950-2012) indicating an approximately linear reduction in the recharge without evident break points. The negative trend of the recharge is 1.8 mm/y, significant at 90% (Figure 3). In Figure 3 also the aquifer discharge from 1997 to 2012, estimated as in paragraph 2.1, is shown.

Preprints (www.preprints.org) | NOT PEER-REVIEWED | Posted: 11 July 2022 doi:10.20944/preprints202207.0163.v1

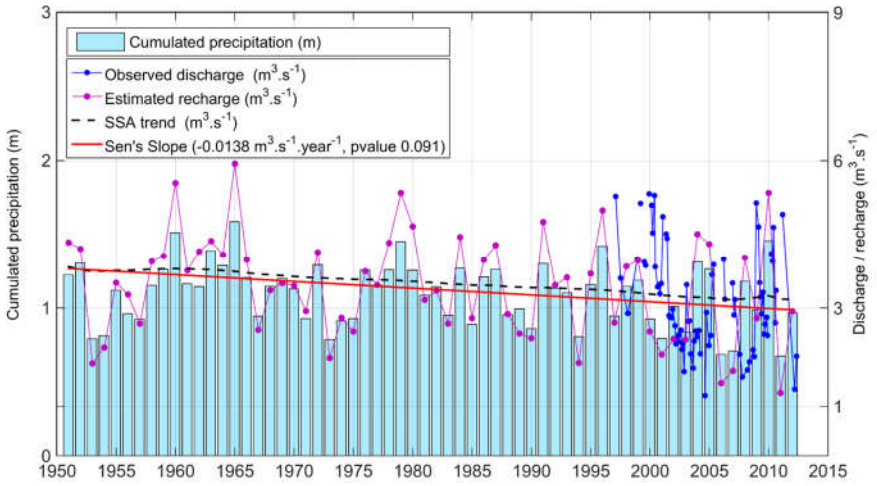

Figure 3. Estimated recharge, with respect to the cumulated precipitation and the observed aquifer discharge.

3. Numerical model description

3.1. Layers discretization, boundary conditions and codes

The steady state models were implemented by gradually increasing the number of layers, from a 1 Layer (2D) to a 3 Layers (Quasi-3D) and then a 5 Layers model (Fully-3D) with uniform grid spacing of 100x100 meters (Figure 4). Top and bottom of the layers were built using the available geological data (boreholes stratigraphy, geological maps, cross sections), by means of an Ordinary Kriging algorithm, with spherical semivariogram. No-flow boundary conditions were assigned to the external boundary of the models. In the Quasi-3D and Fully-3D models, because the upper layers do not cover the whole extent, no-flow boundary conditions (inactive cells) were assigned in the areas where the anticline is eroded (eastern portion), leading the lowermost layers to outcrop. This allows partitioning the recharge into the different layers according to the geological setting, assigning the calculated recharge rates to each outcropping cell. Drain and river packages (DRN and RIV) were used to simulate head dependent flux boundary conditions, for the springs and the Nera River and Precetto stream respectively. Initial hydraulic conductivity and transmissivity values were set based on the available on-site tests and on the results of the previous numerical simulations ([30], [41]). The 2D model features one layer only. Simulating a unique aquifer, it neglects the behaviour of the two aquitards. The groundwater flow is only in the x-y direction. The hydraulic conductivity values (K_h) were set for each cell by considering the average aquifer transmissivity, divided by the cell thickness. The Quasi-3D model consists of three layers, representing the sub-aquifers. Aquitards are not explicitly represented; the groundwater flow in each layer is in the x-y direction and exchanges between layers are regulated through vertical conductance, known as vertical leakage term. Vertical leakage is computed by the preprocessor Groundwater Vistas (Environmental Simulations International®) based on the saturated thickness and vertical K assigned to the implicit aquitard layer ([42]). Finally, the Fully-3D approach allows for vertical flow in aquifers and aquitards through the explicit representation of the aquitards. The Fully-3D model was set up with five layers representing the three sub-aquifers and the two aquitards. Initially, the hydraulic conductivity of the explicit aquitards was assumed to be 1/100 of the hydraulic conductivity values set to each overlaying sub-aquifer. The mean estimated recharge (3.5 m^3/s, see section 2.2) was uniformly assigned as input recharge to the active cells of the models.

Preprints (www.preprints.org) | NOT PEER-REVIEWED | Posted: 11 July 2022 doi:10.20944/preprints202207.0163.v1

2D and Quasi-3D models were run using MODFLOW 88/98 with Preconiugated Gradient 2 solver. In the Fully-3D model, in order to overcome dry-cell problems and reduce the model error, the Newton-Raphson formulation for MODFLOW-2005 (MODFLOW2005-NWT, [23]) was invoked. MODFLOW2005-NWT uses an alternative formulation of the GW-flow equation: the Upstream Weighting Package (UPW) treats nonlinearities of cell drying and rewetting by using a continuous function of hydraulic head, instead of the discrete approach applied by the BCF and LPF packages in the previous MODFLOW versions. Application of MODFLOW-NWT overcomes numerical problem by smoothing the transition from wet to dry cells and keeps all cells active ([43]). MODFLOW-NWT keeps all cells active that are active at the start of the simulation. It assigns a head to unconfined cells even when the head falls below the cell bottom, allowing vertical flow in the form of recharge. However, dry cells no longer participate in horizontal aquifer flow. Use of MODFLOW2005-NWT avoids solver instability in the presence of dry cells and diminishes the sensitivity of the solution to initial conditions.

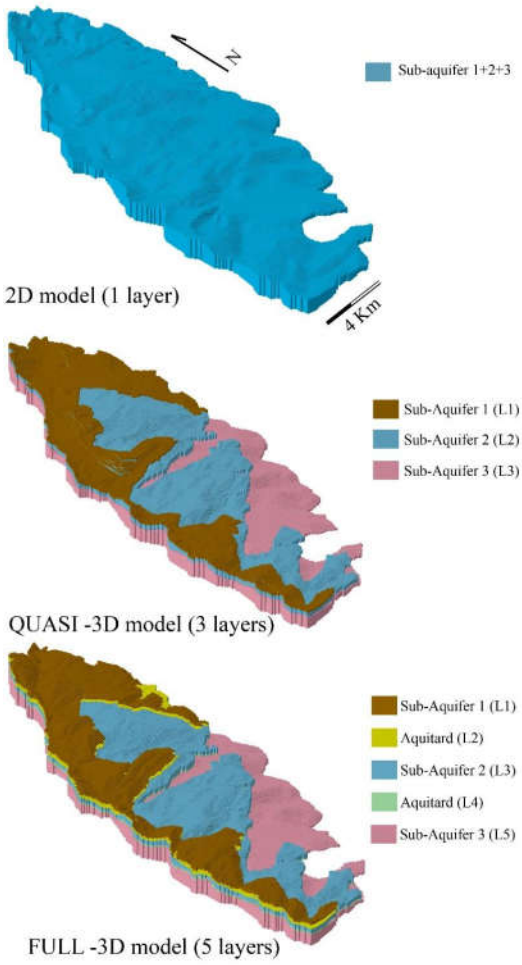

Figure 4. Sketch of the three steady state models implemented with 2D, Quasi-3D and Fully-3D setting. Only active cells are shown.

In order to allow for a robust comparison of the 2D and Quasi-3D simulations to the Fully-3D model, an equivalent transmissivity was calculated for each cell for the Quasi-3D and 2D models, taking account of the reduced number of layers:

$$T_1 + T_2 + T_3 + T_4 + T_5 = T_1, + T_2, + T_3, = T_{2D} = K_1e_1 + K_2e_2 + K_3e_3 + K_4e_4 + K_5e_5 = K_1,e_1, + K_2,e_2, + k_3,e_3, = k_{2D}e_{2D}$$

Preprints (www.preprints.org) | NOT PEER-REVIEWED | Posted: 11 July 2022 doi:10.20944/preprints202207.0163.v1

(Equation 1)

- T_1, T_2, T_3, T_4, T_5 = transmissivity of the Fully-3D model (subscript indicates the layer)
- $T_{1'}$, $T_{2'}$, $T_{3'}$ = transmissivity of the Quasi-3D model (subscript indicates the layer)
- T_{2D} = transmissivity of the 2D model
- K_n = permeability (subscript indicates the layer)
- e_n = thickness (subscript indicates the layer)

3.2. Model calibration

Models were calibrated in steady state through a manual trial-and-error procedure, using the available data, which comprise:

- the discharge increment in Nera River reaches R1 to R4;
- the discharge of Precetto stream;
- the discharge of springs Lupa, Scheggino and Pacce (Table 1).
- the head measured in two wells (Renari di Capriglia and Scheggino, figure 1)

Flux and head targets used for model calibration are listed in Table 2. The topography elevation, especially in deep gorges, where the lower sub-aquifers are outcropping, provided additional head constraints. Calibrated parameters were the horizontal and vertical hydraulic conductivities of each layer and river-bed hydraulic conductivity and thickness (tables 3 and 4). The streambed conductance, which enters in the computation of the groundwater - surface water interaction, is computed by the software as the ratio of riverbed hydraulic conductivity and thickness.

Table 2. Flux and head targets used for model calibration.

Layer	Head target	Flux target
1 (sub-aquifer 1) Scaglia unit	n.a.	Nera River reach R1, Lupa spring, Scheggino spring, Precetto stream
3 (sub-aquifer 2), Maiolica unit	Scheggino well	Nera River reach R2, R3 and R4, Pacce spring
5 (sub-aquifer 3), Calcare massiccio and Corniola	Renari di Capriglia well	n.a.

The calibration phase involved an iterative refining of aquifer K values and distribution and of riverbed K and thickness values, on the basis of a comparison between simulation results and observations. The calibration of hydraulic conductivity in each layer was performed by gradually modifying the K values by "zones", each zone representing a homogeneous area of the layer. At first, the values from [30] were assigned to the sub-aquifers of the Fully-3D model. During the calibration phase, the number of hydraulic conductivity zones was increased in order to refine the k distribution, until the simulated values were close to the observations. After each K value variation, the model was re-run to compare results with the previous setting. Then, the pattern of k values was progressively refined, and many different k zones were added. The most difficult task was to reproduce the discharge of the river and maintain a sufficient discharge in the upper reaches. In order to reproduce this discharge distribution, a high conductivity strip was added, oriented N-S in Layer 5 of the Fully 3D model, which simulates faults bounding Calcare Massiccio Fm, acting as a preferential flow zone. The transmissivity distribution

Preprints (www.preprints.org) | NOT PEER-REVIEWED | Posted: 11 July 2022 doi:10.20944/preprints202207.0163.v1

resulting in the Fully-3D model after this calibration was transposed to the Quasi-3D and 2D models following the equation (1). 2D and Quasi-3D models were further calibrated after this step in order to seek for the best match with observations. In the final setting, the number of calibrated conductivity zones is 3, 6 and 12 for the 2D, Quasi-3D and Fully-3D models, respectively (Table 3, Figure 5). Time of calculation ranges from a few seconds for the 2D model to several minutes for the Fully-3D.

Table 3. range of calibrated Kx, Ky, Kz values.

Model setting	N of layers	N of active cells	N of calibrated K zones	Range of Kx,Ky values, m/s	Range of Kz values , m/s
2D	1	23248	3	1.1E-5/2.8E-5	1.15E-6/2.8E-6
Quasi-3D	3	50959	6	0.1E-6/4.6E-5	1.1E-7/2.8E-6
Fully-3D	5	77212	12	1.1E-6/8.1E-5 (high K strip: 5.7E-4 m/s)	1.1E-7/8.1E-5 (high K strip: 6.3E-4 m/s)

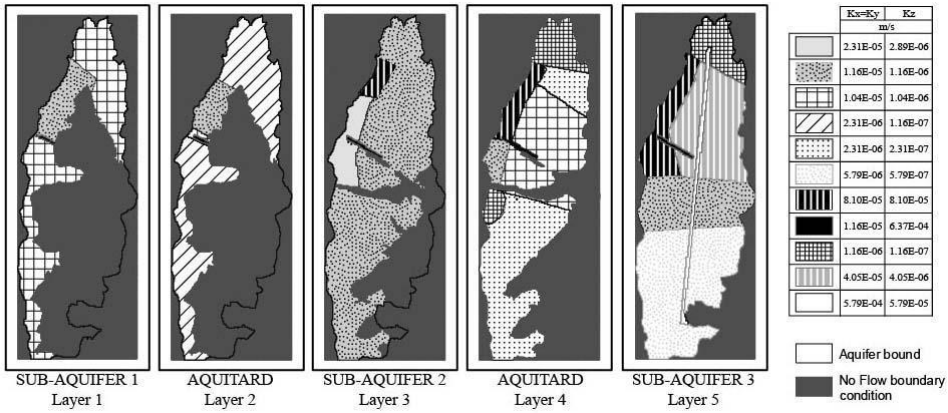

Figure 5. Distribution of K zones for Fully-3D calibrated model.

Table 4. Initial and calibrated values of riverbed hydraulic conductivity and thickness.

River reach	Riverbed Kv (m/s)		Riverbed thickness (m)	
	initial	calibrated	initial	calibrated
1-4 (Nera River)	5.7E-6	2.3E-5	0.1	0.03
5 (Precetto stream)	5.7E-6	2.3E-5	0.1	0.03

4. Results and discussion

All the calibrated models give a good match between simulated and observed heads in the two only available wells. However, the 2D model was never able to match the observed distribution of river baseflow along each Nera River's reach. In fact, assuming a single aquifer, this model is not able to feed the upstream cells of the river and the groundwater converges toward the most downstream RIV cells (Figure 7A), which does not correspond to the observed groundwater-surface water interaction. The upstream reach R1 (Figure 1) loses water to the aquifer instead of gaining, while the downstream reach R4 gains the double of the observed discharge (Table 5).

Preprints (www.preprints.org) | NOT PEER-REVIEWED | Posted: 11 July 2022 doi:10.20944/preprints202207.0163.v1

Table 5. Results of the three models and comparison with the observed values. The bias % is shown

element	observed	2D	Quasi-3D	Fully-3D
Well S., m a.s.l.	273	271.51	275.57	273.26
Well R., m a.s.l.	301	269.88	312.52	305.00
Nera R., R1, l/s	436	-322.00	351.92	238.56
Nera R., R2, l/s	1120	1557.82	812.62	778.68
Nera R., R3, l/s	1110	507.18	751.17	1445.15
Nera R., R4, l/s	609	1173.95	1760.49	669.35
springs, l/s	390	587.99	195.44	286.21
Precetto s., l/s	120	60.40	117.71	103.29

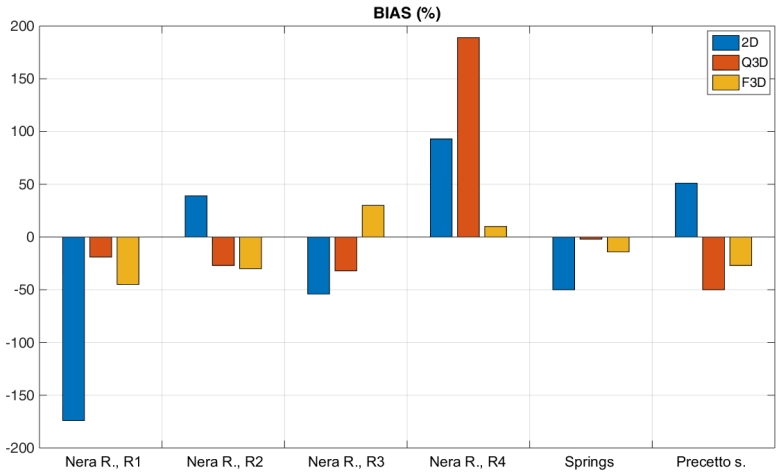

Figure 6. Target bias on the discharge (%).

In order to reproduce the discharge correctly partitioned along the reaches, it was necessary to construct multi-layer models with consideration of system aquitards.

An important advantage of Quasi-3D and Fully-3D models with respect to the 2D model is that the slope and dipping of single layers can be correctly reproduced, allowing flow to be reliably simulated along the layers. In addition, the Quasi-3D and Fully-3D models allow to represent localised areas of preferential upward flow with a non-uniform vertical leakage array or by adding high vertical permeability zones, to simulate discontinuities in the aquitards, respectively.

Further, the Quasi-3D and Fully-3D models allow partitioning the recharge into the different numerical layers according to the geological setting. For example, where the anticline is eroded the recharge is assigned to the outcropping layers, thus each of the sub-aquifers directly receive a share of the total recharge (Figure 4). In the Quasi-3D and Fully-3D models, the simulations show that a large part of the anticline hosts dry cells due to the high elevation of the aquifer bottom with respect to the calculated heads. When using the PCG solver (Quasi-3D model), the dry cells are excluded from the head calculations and recharge is passed to an underlying active cell. Conversely, in the NWT Upstream weighting package (Fully-3D model), dry cells remain active with a calculated head value that falls below the bottom of the cell; that head is used to set up the gradient to pass recharge to an underlying cell hosting the water table or toward adjacent cells in the case of the bottom layer. In particular, the Quasi-3D model performs better than the 2D, but still the simulated discharge of the reach R4 is not acceptable (Table 5). The Fully-3D model shows the best performance in terms of bias (Figure 6). The hydraulic heads calculated for the three aquifers in the Fully-3D (Figure 7B) show the important role of the

 doi:10.20944/preprints202207.0163.v1

basal sub-aquifer (layer 5) to direct the high infiltration from the mountainous recharge areas to the northern, downstream, sectors of the structure. Due to the complex geometry, sub-aquifers 1 and 2 show extended dry cells areas and the head potentials are strongly influenced by the RIV cells.

Indeed, the use of 5 layers allows for a very detailed setting of k zones distribution which, once calibrated, should reflect a possible pattern of permeability values, making the model results consistent with the observed discharge rates and heads. In particular, the insertion of the high conductivity strip in the sub-aquifer 3 (Figure 5) ameliorated by far the calibration of the Fully-3D model. The high hydraulic conductivity zones, thus, are likely to reflect fractures or faults zones. Tectonics also drive the vertical exchanges among the sub-aquifers through the aquitards. A better match was achieved considering zones of relatively high vertical permeability within the aquitards, simulating highly tectonized zones or stratigraphic gaps, for example in correspondence of reach R2 (Figure 5) which allows the groundwater to flow vertically upward from layer 5 to the upper layers.

However, high hydraulic conductivity zones alone were not sufficient to maintain the hydraulic gradients steep enough to feed the most upgradient reach R1. The groundwater flows mostly in the sub-aquifer 3. Despite a prevalent diffuse circulation (which justifies the EPM approach), the high hydraulic conductivity strip along the anticline axis, that facilitates the groundwater to flow from south to north, is consistent with a discrete groundwater circulation pattern. This was confirmed by observation during the perforation of the Renari well for the Calcare Massiccio aquifer, which showed a prevalent circulation through fractures. Table 5 lists the results of the three models after calibration. Figure 6 shows the bias %.

Ultimately, the calibration process points to the presence of structural elements in the flow system that are not readily observable by other means. In this sense the stepwise process is not meant to produce a unique representation of the subsurface, but rather points to the existence of subsurface features that seem to be controlling flow to the river according to the fully 3D model, but which are otherwise very difficult to characterize by field work, i.e. examination of outcrops or geophysical prospections. Such a model can be considered as an interpretive model ([44]), in the sense of a screening model that helps the modeler to develop an initial understanding of a groundwater system and/or test hypotheses about the system. Calibration through manual trial-and-error proved that a simple 2D model is not able to match field observations and thus is not an acceptable model for the site. Further, it allowed to get insight on how parameter changes in different areas of the model could correspond to subsurface unknown features ([44]). For example, the high permeability strip in the deepest layer in the Fully-3D model could suggest the existence of a developed still unknown karstic system. This manual process, although seemingly unable to find a unique solution, might be the only way forward, given the impossibility of quantifying the "true uncertainty" in natural systems and the error inevitably associated with a complex structural model with few data supporting observations ([45]). As stated by Fienen at al., 2009 [46], parsimonious models should avoid unnecessary or unsupported complexity while accurately delineating flow paths given our state of knowledge about the field setting.

Preprints (www.preprints.org) | NOT PEER-REVIEWED | Posted: 11 July 2022 doi:10.20944/preprints202207.0163.v1

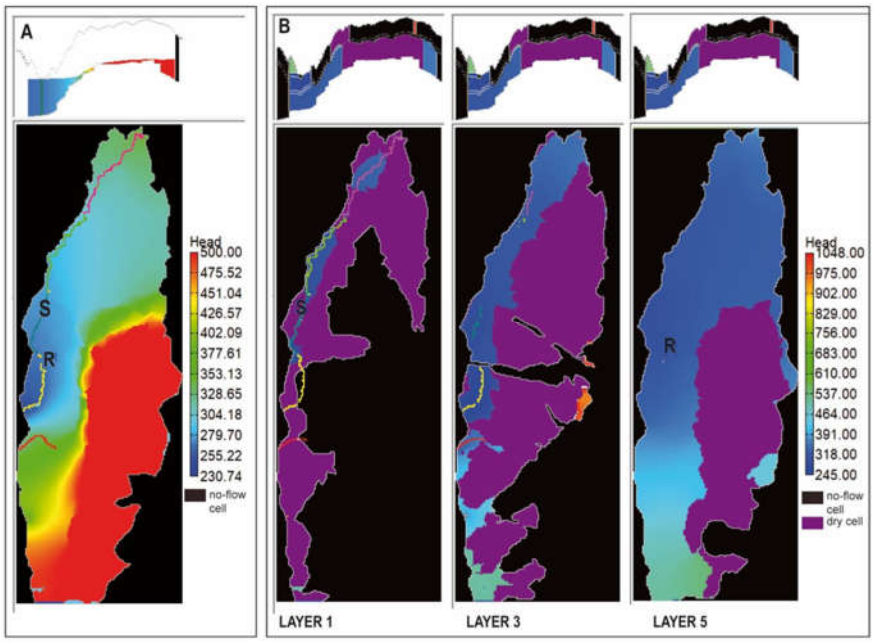

Figure 7. Simulated head for the 2D model (A) and for the layers 1, 3 and 5 in the Fully-3D model (B). Model cross sections at the top of figures (row 162, column 23).

5. Conclusions

Modelling a complex structure-dictated hydrogeological system requires a stepwise procedure to reach the best solution with a parsimonious model setting. The inherent complexity of the conceptual model was reproduced in the numerical model by progressively adding elements to the model grid (such as new layers from the 2D to the Fully-3D) or hydraulic conductivity zones, and calibrating by manual trial-and-error the steady state solution. Furthermore, gradually increasing the model complexity can be a useful approach for simulating groundwater flow when few head data are available as it is common in karst aquifers). Due to the prevalent diffuse circulation, an EPM approach was used; however, the calibrated setting of hydraulic conductivity zones suggests a discrete groundwater circulation pattern, which was successfully simulated by adding a high permeability longitudinal strip. The calibrated pattern of K zones both for sub-aquifers and aquitards, is likely to reflect the structural and stratigraphic setting. The Quasi-3D and the Fully-3D both allow for the recharge partitioning into the sub-aquifers. The vertical exchanges among the sub-aquifers are regulated by leakage coefficient or aquitards parametrization, respectively. The higher number of layers with respect to the 2D model allows the 3D simulations to drive the groundwater flow towards the different parts of the river. However, the Fully-3D model best matches the observed flow distribution at the different reaches along the river, simulating reliable flow paths and recharge partitioning into layers. The Newton-Raphson formulation of MODFLOW2005 is required, to achieve convergence and reduce model error mainly due to cells drying and rewetting producing numerical instabilities. The numerical model demonstrated the major impact of folded and faulted geological structures on controlling the flow dynamics in terms of flow direction, water heads and spatial distribution of the outflows to the river and springs. The stepwise process of model construction and calibration, even with a limited number of head and flux targets, points to the presence of structural elements in the subsurface that otherwise can escape observation in field studies of the terrain.

Author Contributions: Conceptualization, E.P. and C.D.S.; methodology, E.P., C.D.S., N.G. E.R.; software, E.P., C.D.S., A.P., N.G.; validation, E.P., C.D.S., E.R.; formal analysis, E.P., C.D.S., E.R.; investigation, E.P., C.D.S.; resources, E.P.; data curation, E.P., C.D.S.; writing—original draft preparation, E.P., C.D.S.; writing—review and editing, E.P., C.D.S, ER.; visualization, C.D.S., A.P., E.R., N.G.; supervision, E.P.; All authors have read and agreed to the published version of the manuscript." Please turn to the CRediT taxonomy for the term explanation.

Funding: This research received no external funding

Data Availability Statement: Data of springs discharge and have been provided by the Regional Agency for Environmental Protection (ARPA Umbria). Precipitation, temperature and river discharge data have been provided by the Hydrographic Service of Umbria (Ufficio Idrografico della Regione Umbria).

Acknowledgments: The authors are deeply grateful to Daniel Feinstein and Rundy Hunt (USGS) for their useful suggestions and review of the manuscript.

Conflicts of Interest: The authors declare no conflict of interest.

References

1. Ford D.C.; Williams P.W. *Karst hydrogeology and geomorphology*. Wiley, Chichester, **2007**, 562 pp
2. Worthington, S.R.H., Ford, D.C. Self-organized permeability in carbonate aquifers. Ground Water **2009**, *37(3)*, 326–336
3. Worthington, S.R.H. Management of Carbonate Aquifers, In: *Karst Management*, Van Beynen, P. E., Eds.; Dept. Geography, University of South Florida, Tampa, USA, 2011, XII, pp. 243-261, DOI 10.1007/978-94-007-1207-2
4. W. Dragoni, W., Mottola, A., Cambi, C., Modeling the effects of pumping wells in spring management: the case of Scirca spring (central Apennines, Italy),*J. Hydrol.* **2013**, *493*, 115-123
5. Fiorillo, F.; Guadagno, F.M. Karst Spring Discharges Analysis in Relation to Drought Periods, Using the SPI. *Water Resources Management* **2010**, *24*, pp. 1867–1884. https://doi.org/10.1007/s11269-009-9528-9
6. Romano, E., Preziosi, E. Precipitation pattern analysis in the Tiber River basin (central Italy) using standardized indices. *International Journal of Climatology* **2013**. *33 (7)*, 1781-1792 doi: 10.1002/joc.3549
7. Citrini, A.; Camera, C.; Beretta, G.P. Nossana Spring (Northern Italy) under Climate Change: Projections of Future Discharge Rates and Water Availability. *Water* **2020**, *12*(2), 387; https://doi.org/10.3390/w12020387
8. Leone, G.; Pagnozzi, M.; Catani, V.; Ventafridda, G.; Esposito, L.; Fiorillo, F. A hundred years of Caposele spring discharge measurements: trends and statistics for understanding water resource availability under climate change. *Stoch Environ Res Risk Assess* **2021**, *35*, pp. 345–370. https://doi.org/10.1007/s00477-020-01908-8
9. Romano, E., Petrangeli, A.B., Salerno, F., Guyennon, N. Do recent meteorological drought events in central Italy result from long-term trend or increasing variability? International Journal of Climatology **2021**, *42*, 4111–4128. doi: 10.1002/joc.7487
10. Romano, E., Preziosi, E., Petrangeli, A.B.. Spatial and Time Analysis of Rainfall in the Tiber River Basin (Central Italy) in relation to Discharge Measurements (1920-2010). *Procedia Environmental Sciences* **2011**, 258–263. doi:10.1016/j.proenv.2011.07.045
11. IPCC 2022 - Climate Change 2022: Impacts, Adaptation, and Vulnerability. Contribution of Working Group II to the Sixth Assessment Report of the Intergovernmental Panel on Climate Change [H.-O. Pörtner, D.C. Roberts, M. Tignor, E.S. Poloczanska, K. Mintenbeck, A. Alegría, M. Craig, S. Langsdorf, S. Löschke, V. Möller, A. Okem, B. Rama (eds.)]. Cambridge University Press.
12. Preziosi E., Romano, E., Are large karstic springs good indicators for Climate Change effects on groundwater? *Geophysical Research Abstracts* **2013**, 15, 9367. Proceedings of the European Geosciences Union General Assembly 2013, Vienna, Austria, 7-12 April 2013.
13. Romano E., Del Bon, A., Petrangeli, A.B., Preziosi, E. Generating synthetic time series of springs discharge in relation to standardized precipitation indices. Case study in Central Italy. *Journal of Hydrology* **2013**, *507*, 86–99. doi: 10.1016/j.jhydrol.2013.10.020
14. European Community, Directive 2000/60/EC of the European Parliament and of the Council of 23 October 2000 establishing a framework for Community action in the field of water policy, https://eur-lex.europa.eu/LexUriServ/LexUriServ.do?uri=CELEX:32000L0060:EN:HTML, last accessed 5 July 2022
15. Gattinoni, P., Francani, V. Depletion risk assessment of the Nossana Spring (Bergamo, Italy) based on the stochastic modelling of recharge. *Hydrogeol J* **2010**, *18*,325–337
16. Levinson, J.; Larocque, M.; Ouellet, M.A. Modeling low-flow bedrock springs providing ecological habitats with climate change scenarios. *Journal of Hydrology* **2014**, *515*, pp. 16-28
17. Reimann, T., Giese, M., Geyer, T., Liedl, R., Marechal, J.C., Shoemaker, W.B. Representation of water abstraction from a karst conduit with numerical discrete-continuum models, *Hydrol. Earth Syst. Sci.* **2014**, 18, 227-241,. doi:10.5194/hess-18-227-2014.

18. Scanlon, B.R., Mace, R.E., Barrett, M.E., Smith, B. Can we simulate regional groundwater flow in a karst system using equivalent porous media models? Case study, Barton Springs Edwards aquifer, USA. *Journal of Hydrology* **2003,** *276,* 137–158.
19. Abusaada, M.; Sauter, M. Studying the Flow Dynamics of a Karst Aquifer System with an Equivalent Porous Medium Model. *Groundwater* **2013**, *51*, pp. 641–650
20. Ben-Itzhak, L.; Gvirtzman, H. Groundwater flow along and across structural folding: an example from the Judean Desert, Israel. *J Hydrol* **2005**, *312*, pp. 51-69
21. Dafny, E.; Burg, A.; Gvirtzman H. Effects of karst and geological structure on groundwater flow: the case of Yarqon-Taninim Aquifer, Israel. *Journal of hydrology* **2010,** *389*, pp. 260-275.
22. Valota, G., Giudici, M., Parravicini, G., Ponzini, G., Romano, E. Is the forward problem of Ground Water Hydrology always well posed?, *Ground Water* **2002**, *40 (5)*, 500-508
23. Niswonger, R.G., Panday, S., Ibaraki, M. MODFLOW-NWT, A Newton formulation for MODFLOW-2005: U.S. Geological Survey Techniques and Methods 6-A37, **2011**, 44 p.
24. Mantoglou, A., On optimal model complexity in inverse modeling of heterogeneous aquifers, *Journal of Hydraulic Research* **2015**, *43 (5)*, 574-583
25. Hill M. C. The practical use of simplicity in developing groundwater models. *Ground Water* **2006** *44(6)*, pp. 775–781.
26. Moore, C., Wöhling, T., Doherty, J. Efficient regularization and uncertainty analysis using a global optimization methodology, *Water Resour. Res.* **2010**, 46 W08527, doi:10.1029/2009WR008627.
27. Hill M.C. Methods and guidelines for effective model calibration, *U.S. Geological Survey, water-resources investigations report* **1998**, *98-4005*.
28. Barchi, M.R.; Lemmi, M. Geology of the area of Monte Coscerno-Monte di Civitella (South-eastern Umbria). *Boll. Soc. Geol. It.* **1996**, *115*, pp. 601-624.
29. Boni, C.; Preziosi, E. Una possibile simulazione numerica dell'acquifero basale di M.Coscerno - M.Aspra (bacino del fiume Nera). *Geol.Appl. e Idrogeologia* **1993**, *28*, pp. 131-140, Bari.
30. Preziosi E., 2007, Simulazioni numeriche di acquiferi carbonatici in aree corrugate: applicazioni al sistema idrogeologico della Valnerina (Italia centrale). *Quad IRSA-CNR, Istituto di Ricerca sulle Acque-CNR,* 125, ISSN 0390-6329, pp. 225
31. Mastrorillo, L., Baldoni, T., Banzato, F., Boscherini, A., Cascone, D., Checcucci, R., Petitta, M., Boni, C. Quantitative hydrogeological analysis of the carbonate domain of the Umbria Region (Central Italy), *Italian Journal of Engineering Geology and Environment* **2009,** *1,*137–155. doi: 10.4408/IJEGE.2009-01.O-08
32. Mastrorillo, L; Petitta, M. Hydrogeological conceptual model of the upper Chienti River Basin aquifers (Umbria-Marche Apennines), *Italian Journal of Geosciences* **2014,** *133 (3)*, 396–408., https://doi.org/10.3301/IJG.2014.12
33. Di Matteo, L.; Dragoni, W.; Ulderico, V.; Latini, M.; Spinsanti, R. Risorse idriche sotterranee e loro gestione: il caso dell'ATO2 Umbria (Umbria meridionale). *Acque sotterranee* **2005**, *96*
34. ARPA Umbria. Available on line: https://apps.arpa.umbria.it/acqua/contenuto/monitoraggio-in-continuo-acque-sotterranee (accessed on 13 June 2022)
35. Preziosi, E., Romano, E., From hydrostructural analysis to mathematical modelling of regional aquifers. *Italian Journal of Engineering Geology and Environment* ***2009***, *1*, 183-198. ISSN 1825-6635. doi: 10.4408/IJEGE.2009-01.O-10
36. ARPA Umbria, Il Sistema Informativo di Arpa Umbria e la Conoscenza Ambientale, a cura di Mauro Emiliano, Quaderni Arpa Umbria 2004. https://www.arpa.umbria.it/pagine/il-sistema-informativo-di-arpa-umbria-e-la-conosce, last accessed 5 July 2022
37. White, W.B., Geomorphology and Hydrology of Karst Terrains. Oxford Univ. Press, New York, 1988, 464 pp
38. Vigna, B., Banzato, C., The hydrogeology of high-mountain carbonate areas: an example of some Alpine systems in southern Piedmont (Italy), *Environ. Earth Sci.* **2015**, *74 (1)*, 267-280
39. Thornthwaite, C.W. Mather, J.R. The water balance. *Climatology* **1955**, *8 (1)*, 5-86
40. Thornthwaite, C.W. Mather, J.R., Instructions and Tables for Computing Potential Evapotranspiration and the Water Balance, *Publ. in Climat.* **1957,** *10* (3), pp. 185-310., Drexel Institute of Technology, Laboratory of Climatology, Philadelphia, Pa
41. ATO Umbria 2 S.I.I. S.c.p.a. UMBRIADUE S.c.a.r.l. SEVERN TRENT ITALIA S.p.a. Acquedotto Scheggino-Pentima, *Progetto definitivo, Relazione tecnica* **2006**
42. Rambaugh, J.O., Rambaugh D.,B, Guide to using Groundwater Vistas, version 7, Environmental Simulation 2017, available at: https://d3pcsg2wjq9izr.cloudfront.net/files/4134/download/730323/4-gv7manual.pdf, last accessed 5 July 2022
43. Feinstein, D.T.; Fienen, M.N.; Kennedy, J.L. Development and application of a groundwater/surface-water flow model using MODFLOW-NWT for the Upper Fox River Basin, Southeastern Wisconsin *U.S. Geological Survey Scientific Investigations Report* **2012**, *5108*
44. Anderson, M.P.; Woessner, W.W.; Hunt, R.J. *Applied Groundwater Modeling: Simulation of Flow and Advective Transport*, 2nd ed.; Academic Press, Inc., 2015; 564 p. ISBN 9780120581030.
45. Hunt, R.J. Applied Uncertainty. *Groundwater* **2017**, *55(6)*, pp.771-772. http://dx.doi.org/10.1111/gwat.12604.
46. Fienen, M.F.; Hunt, R.J.; Krabbenhoft, D.P.; Clemo, T. Obtaining parsimonious hydraulic conductivity fields using head and transport observations: A Bayesian Geostatistical parameter estimation approach. *Water Resources Research* **2009**, *45*, W08405, doi: 10.1029/2008WR007431

 doi:10.20944/preprints202207.0163.v1